20 µm gate width CVD graphene FETs for 0.6 THz detection

20 μm gate width CVD graphene FETs for 0.6 THz detection

Audrey Zak[1], Michael A. Andersson[1], Maris Bauer[2], Alvydas Lisauskas[2], Hartmut G. Roskos[2] and Jan Stake[1]
[1]Chalmers University of Technology, SE-412 96 Gothenburg, Sweden
[2]Johann Wolfgang Goethe Universität, Frankfurt am Main, Germany

***Abstract*—We have fabricated 20 μm gate width graphene field effect transistors (GFETs) based on graphene grown by chemical vapor deposition (CVD). These GFETs are integrated with split bow-tie antennae for room temperature, direct detection of a 0.6 THz signal. Our detectors reach a maximum optical responsivity of 3.0 V/W and a minimum noise-equivalent power (NEP) of 700 pW/Hz$^{0.5}$. The successful demonstration of THz detection using CVD graphene introduces the possibility for scalable detector production.**

I. INTRODUCTION

PROGRESS toward bridging the so-called 'terahertz gap' has been thus far limited by the availability of high frequency detectors and emitters [1]. Terahertz applications require materials with high mobilities, and for practical devices, operation at room temperature is desired. Graphene, a two-dimensional semimetal, has been found to have room-temperature carrier mobilities up to 10,000 cm^2 V^{-1} s^{-1} [2] on SiO_2. The high carrier mobility of graphene coupled with the demonstration of self-mixing in materials with electrons confined to two-dimensions [3], [4] suggests that GFETs have potential as terahertz detectors.

While mechanically exfoliated graphene has been used for room-temperature terahertz detection [5], [6], graphene grown by chemical vapor deposition (CVD) has not been similarly studied. Furthermore, integration of a CVD graphene FET with a bow-tie antenna for high frequency detection is as yet unexplored with this type of GFET design [7].

Our detectors were fabricated with a split bow-tie antenna design where the antenna bows act as the GFET electrodes, simultaneously applying gate bias as well as allowing read-out of the rectified signal at the drain. Graphene is grown by CVD and transferred to Si/SiO_2 substrates. Source and drain electrodes are patterned with electron beam lithography followed by Ti/Pd/Au metallization. The graphene outside the channel area is etched away and 15 nm Al_2O_3 gate oxide is deposited by atomic layer deposition. Finally, gate metal and probing pads for device measurement are patterned. Fig. 1 shows an SEM image of a detector as well as the measurement setup. Three GFET designs were fabricated, with gate lengths of 250, 500, and 1000 nm and a gate width of 20 μm.

II. RESULTS

The overall drain-source resistance of the GFETs was measured and is shown in Fig. 2(a) for each of the three GFET designs. As expected, the GFET with the longest gate length had the highest resistance level. From the drain-source resistance R_{DS} the transconductance g_m was calculated as the derivative of the source-drain current with respect to the gate voltage at constant drain bias, shown in Fig. 2(c). The transconductance changes sign near the Dirac voltage (the gate voltage where R_{DS} is a maximum) indicating the transition between holes and electrons as majority carriers.

The optical voltage response R_V was measured using lock-in

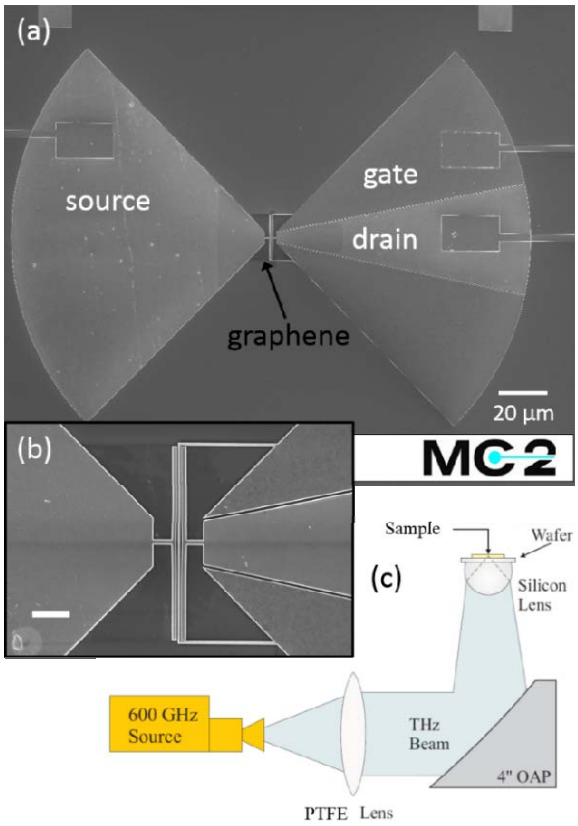

Fig. 1. (a) SEM image of bow-tie antenna coupled to GFET with source, drain, and gate labeled. The graphene is visible as a dark shadow on the substrate (b) Zoom of GFET, gate width = 20 μm, gate length = 250 nm, scale bar is 4 μm. (c) Setup for measurement at 0.6 THz where the beam is focused by a PTFE collimating lens, then directed to the sample with an off-axis parabolic (OAP) mirror. The detectors are mounted on a silicon wafer on top of a silicon lens for further beam focusing.

detection for a square-wave modulated (at 333 Hz), 0.6 THz beam with a measured power of 290 μW. From the voltage response, the optical voltage responsivity $\Re_V$ was calculated as

$$\Re_V = \frac{\pi}{\sqrt{2}} \frac{R_V}{P},$$

where the numerical pre-factor is a consequence of lock-in detection and square-wave beam modulation, and P is the power incident on the antenna. The total beam power was considered in the calculation of the responsivity, meaning that the values calculated are conservative estimates as not all of the beam power was coupled to the GFET due to optical losses and antenna-device impedance mismatch. The responsivity of

a detector of each gate length is shown in Fig. 2(b) and is found to be independent of chopper modulation frequency in the range of 33 Hz – 3.3 kHz.

The NEP of each of the detectors is calculated as

$$NEP = \frac{N}{\Re_V} = \frac{\sqrt{4k_B T R_{DS}}}{\Re_V}.$$

The noise in the detectors is assumed to be thermal Johnson noise, dependent on the temperature T and drain-source resistance, because all measurements were made with zero drain-source bias and the gate leakage current was less than 1 nA. The minimum values of the NEP for each gate length are summarized in TABLE I. As with the calculation of the responsivity, the values calculated for the NEP are upper limits.

TABLE I. Responsivity and NEP

Gate length	max. $\Re_V$ (V/W)	min. NEP (pW/Hz$^{0.5}$)
250 nm	1.9	890
500 nm	2.6	700
1000 nm	3.0	760

Rectification of a THz signal can occur through classical resistive mixing in the FET channel, where a coupling capacitance connects the gate and drain. At high frequencies, detection can be through distributed resistive mixing [4], where the dc signal generated is enhanced by plasma wave generation [3]. Preliminary modeling of our detectors using a standard circuit simulation indicates that the operation of the devices was in the distributed mixing regime of THz detection.

The short gate length and wide gate width made efficient modulation of the drain-source resistance possible. It was expected that larger transconductance would lead to higher responsivity, but in fact this was not the case. It was instead the detector with the longest gate length (1000 nm) and the highest overall resistance that had the largest maximum responsivity even though it did not record the highest transconductance. In the calculation of NEP, the overall resistance impacts the noise, which means that there is a trade-off between the drain-source resistance and the responsivity. The GFET with a gate length of 500 nm had a low R_{DS} and good responsivity, resulting in the lowest NEP and therefore the most sensitive detection.

Using a top gated GFET integrated with the bow-tie antenna where the source-gate and gate-drain separation was only 100 nm so as to keep parasitic resistance low, our NEPs were much lower than previous work with graphene [5], [6], [8]. However, a comparison with minimum NEPs of established room temperature detector technologies shows that our detectors are still an order of magnitude higher than state-of-the-art technologies like Si MOSFETS (>10 pW/Hz$^{0.5}$) [9] and Schottky diodes (20 pW/Hz$^{0.5}$) [10].

III. Summary

In summary, we have successfully fabricated sensitive, room-temperature antenna-integrated THz detectors using CVD graphene. By implementing a wide gate design with a short channel length, we realized efficient modulation of the overall resistance which resulted in good responsivity and ultimately low NEP. The use of large-area CVD graphene demonstrates the scalability of detector production.

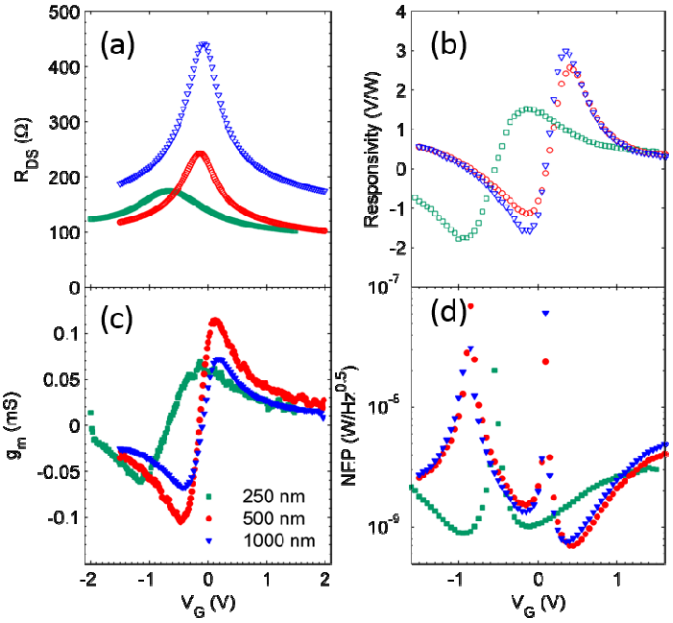

Fig. 2. (a) Drain-source resistance R_{DS} for devices with gate lengths of 250 nm (green squares), 500 nm (red circles), and 1000 nm (blue triangles). (b) Voltage responsivity of detectors from (a) measured at 0.6 THz. (c) Transconductance g_m calculated from R_{DS}. (d) Noise-equivalent power (NEP) calculated from voltage responsivity and source-drain resistance.

References

[1]. M. Tonouchi, "Cutting-edge terahertz technology," *Nature Photonics*, vol. 1, pp. 97-105, Feb. 2007.

[2]. K.S. Novoselov, *et al.*, "Electric field effect in atomically thin carbon films," *Science*, vol. 306, pp. 666-669, Oct. 2004.

[3]. M. Dyanokov and M. Shur, "Detection, mixing, and frequency multiplication of terahertz radiation by two-dimensional electronic fluid," *IEEE Transactions on Electron Devices*, vol. 43, pp. 380-387, Mar. 1996.

[4]. S. Boppel, *et al.*, "CMOS integrated antenna-coupled field-effect transistors for the detection of radiation from 0.2 to 4.3 THz," *IEEE Transactions on Microwave Theory and Techniques*, vol. 60, pp. 3834-3843, Dec. 2012.

[5]. L. Vicarelli, *et al.*, "Graphene field-effect transistors as room-temperature terahertz detectors," *Nature Materials*, vol. 11, pp. 865-871, Oct. 2012.

[6]. D. Spirito, *et al.*, "High performance bilayer-graphene terahertz detectors," *Applied Physics Letters*, vol. 104, 061111, Feb. 2014.

[7]. A. Zak, M.A. Andersson, M. Bauer, A. Lisauskas, H.G. Roskos, and J. Stake, "Antenna-integrated 0.6 THz FET direct detectors based on CVD graphene," unpublished.

[8]. A.V. Muraviev, S.L. Rumyantsev, G. Liu, A.A. Balandin, W. Knap, and M.S. Shur, "Plasmonic and bolometric terahertz detection by graphene field-effect transistor," *Applied Physics Letters*, vol. 103, 181114, Oct. 2013.

[9]. A. Lisauskas *et al.*, "Exploration of terahertz imaging with silicon MOSFETs," *J. Infrared Millim. Te.*, vol. 35, pp. 63-80, 2014.

[10]. L. Liu, J.L. Hesler, H. Xu, A.W. Lichtenberger, and R.M. Weikle, II, "A broadband quasi-optical terahertz detector utilizing a zero-bias Schottky diode," *IEEE Microwave and Wireless Component Letters*, vol. 20, pp. 504-506, Sep. 2010.